 doi:10.20944/preprints201912.0033.v1

Article

Characteristics of the Supercell Cb Thunderstorm and Electrical Discharges on 19 August 2015, North Caucasus: A Case Study

Magomet T. Abshaev [1], Ali M. Abshaev [1,*], Yuriy P. Mikhailovskiy [2], Andrey A. Sinkevich [2], Viktor B. Popov [2] and Anatoliy Kh. Adzhiev [3]

[1] Hail suppression Research Center "ANTIGRAD", 198 Chernishevsky Street, Nalchik 360004, Russia; info@hsrc-antigrad.com (M.T.A.); abshaev.ali@mail.ru (A.M.A.)
[2] Voeikov Main Geophysical Observatory, Saint-Petersburg, Russia; yupalych@yandex.ru (Y.P.M.); sinkevich51@mail.ru (A.A.S.); qoower@gmail.com (V.B.P.)
[3] High Mountain Geophysical Institute, Nalchik, Russia; adessa1@yandex.ru (A.K.A.)
* Correspondence: abshaev.ali@mail.ru; Tel.: +7-928-694-4199 (A.M.A.)

Abstract: The development of extremely powerful thunderstorm originated on the Black Sea Coast on August 19, 2015 and classified as a supercell is discussed in this paper. High depth hail cloud as well as several weaker hailstorms passed more than 1000 km over Northern Caucasus of Russia, the Caspian Sea, and invaded the territory of Kazakhstan. During more than 20 hours this supercell produced heavy hail, rain, intense lightning discharges, gust and tornado which rarely occur in the region. The study of the structure and characteristics of the thunderstorm during the formation of electrical discharges and their frequency were of particular interest. Development of convective clouds and separate thunderstorms were expected, though the powerful hail process was not expected due to small vertical temperature gradients and the absence of cold fronts. Supercell was tracked by 5 radars, which showed its right-hand development with clock-wise deviation from the leading stream on 40-50 degrees and the speed 60-85km/h. Maximum reflectivity factor exceeded value 75dBZ, cloud top reached 15-16km and the height of the hail core rose on 11.2km. The size of hailstones size was 2–3cm, and at the peak of cloud development 4–6 cm. Maximum frequencies of cloud-to-ground flashes of negative and positive polarities reached 30-35min^{-1} and 60-70min^{-1} correspondingly, while frequency of cloud-to-cloud flashes amounted up to 300-500min^{-1}. The maximum frequency of flashes of different types coincided in time. Total current of the cloud-to-ground flashes of positive and negative polarities was almost identical in magnitude and differed by sign (200-300 kA) at the peak of development. The minimum value of radiation temperature, measured by Meteosat-10 satellite in 10.8 μm channel was -60ºC. The most intensive precipitation flux derived from radiometric measurements was about 22000m^3/sec; at the same period radars assessments showed precipitation up to 550mm/h (mixed phase precipitation) and size of hail 4.5cm. The combined satellite-radar-lightning data analysis showed that radar derived characteristics of the supercell reached their maximums earlier than maximum in lightning activity. The highest correlation coefficient between radar and lightning characteristics of the supercell storm was found for pair maximum reflectivity and intensity of LF (0.55) and VHF (0.66) discharges. Estimations of relationship between hail size and lightning activity showed that with increasing hail size, thunderstorm activity increases for both cloud-to-ground and intracloud flashes (on the level 0.46 - 0.59). Analysis of Doppler-polarimetric data showed strong inflow zone associated with tornado. Tornadic debris signature was manifested by radar reflectivity factor Z_H> 60 dBZ, differential reflectivity Z_{DR} > -1 dB, copolar cross-correlation coefficient ρ_{HV} < 0.6, and it was collocated with the tornado vortex signature. Doppler velocities in mesocyclone zone reached values -43 and +63 m/s. Prominent radar echo hook was identified in 1.5 km layer above the ground, while Z_{DR} columns was relatively narrow (4–8 km wide) and not very deep (4.5 km).

 doi:10.20944/preprints201912.0033.v1

Keywords: convective clouds; supercell hailstorm; thunderstorm; lightning; gust; tornado, Meteosat

Abbreviations

Cb - Cumulonimbus cloud;

UTC - Coordinated universal time;

ASL - Above Sea level;

WMO - World Meteorological Organization;

Roshydromet - Russian Hydrometeorological Service;

TV - Television;

SWET - Severe Weather ThrEAT index;

KINX - K index of convective instability;

VTOT - Vertical Totals index;

CTOT - Cross Totals index;

TTOT - Total Totals index;

LIFT - Lifted index;

SHOW - Showalter index;

CAPE - Convective available potential energy;

CIN - Convective Inhibition;

VIL - Vertically integrated liquid, expressed usually in kg/m^2;

LF - Low frequency;

VHF - Very high frequency;

CG - Cloud to ground lightning discharges;

CC - Cloud to cloud lightning discharges;

TDS - Tornadic debris signature;

TVS - Tornado vortex signature.

1. Introduction

This paper discusses the hailstorm which took place on 19 August 2015, when high-depth hail Cb originated on the Black Sea Coast and classified as a supercell as well as several weaker hail clouds passed more than 1000 km through Adygea, Krasnodar, and Stavropol Districts, Karachay-Cherkessia, Kabardino-Balkaria and Dagestan Republics and beyond, forcing the Caspian Sea and invaded the territory of Kazakhstan.

The long lifetime, high values of radar derived characteristics (radar reflectivity, cloud water content, vertically integrated water content) which are rarely observed in nature and high propagation speed were distinctive features of analyzed supercell. Hailfall from supercell was followed by a hurricane wind and tornado. The damage to agro-industrial complex, lines of electro-gas-and water supply, roofs and glasses of buildings, ground transport was estimated as several billion Russian rubles. About 50 people applied for medical treatment.

Since the late 1940s meteorologists have tried to assess thunderstorm risk with the help of thunderstorm indices and parameters that are deduced from the vertical temperature, moisture and wind profiles. Here, most attention is paid to correlations between characteristics derived from radar, satellite and radiosonde measurements with frequencies and currents of lightning discharges.

Preprints (www.preprints.org) | NOT PEER-REVIEWED | Posted: 4 December 2019 doi:10.20944/preprints201912.0033.v1

A wealth of data was gotten for the 19 Aug 2015 thunderstorm. This includes extensive remote sensing data, numerous TV and news reports. Here, the information relevant for the present study is under consideration.

The structure of this article is the following. A brief description of the climatology of investigated region is presented in section 2. Synoptic situation which determined the development of the supercell is presented in section 3. In sections 4-7, we describe the data sets: upper air sounding, radar, lightning and satellite data. Section 8 is devoted for search of pair correlations between radar-lightning and satellite-lightning data, and finally triple radar-satellite-lightning data is analyzed. In section 9, we assess relation between lightning activity and hail size, while section 10 describes tornado features produced by the supercell. Finally, in Section 11, we conclude with a summary of the results and with some recommendations for future research.

2. Climatology

According to recent climate classification by Beck et al. [1] as well as Peel et al [2], the region of concern (Figure 1) refers to humid subtropical climate (Csb - Warm temperate with warm and dry summer) on the west, Humid Continental in the middle southern part (Dfb - Temperate continental climate with hot and warm summers) with hot summers and year round precipitation and cold semi-arid climate (BWh - arid desert) on the east. The amount of annual and monthly average rainfall in the period 1991–2016 is presented in Figure 2, it varies tremendously for different parts of selected area [3]. Monthly precipitation for western part (Figure 2a) is around 80 mm in August, 45 mm for central part (Figure 2b) and 36 mm for eastern part (Figure 2c). August is characterized as the warmest month for all three areas.

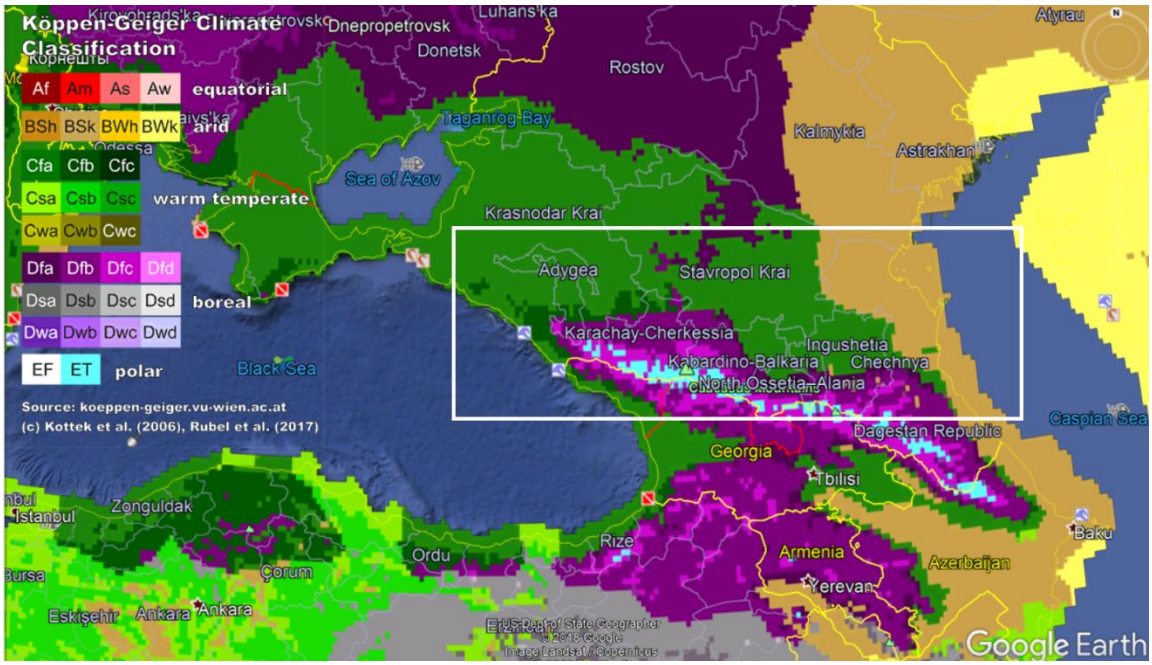

Figure 1. Three climate types bounded by white rectangle of the investigated region (Northern Caucasus).

Preprints (www.preprints.org) | NOT PEER-REVIEWED | Posted: 4 December 2019 doi:10.20944/preprints201912.0033.v1

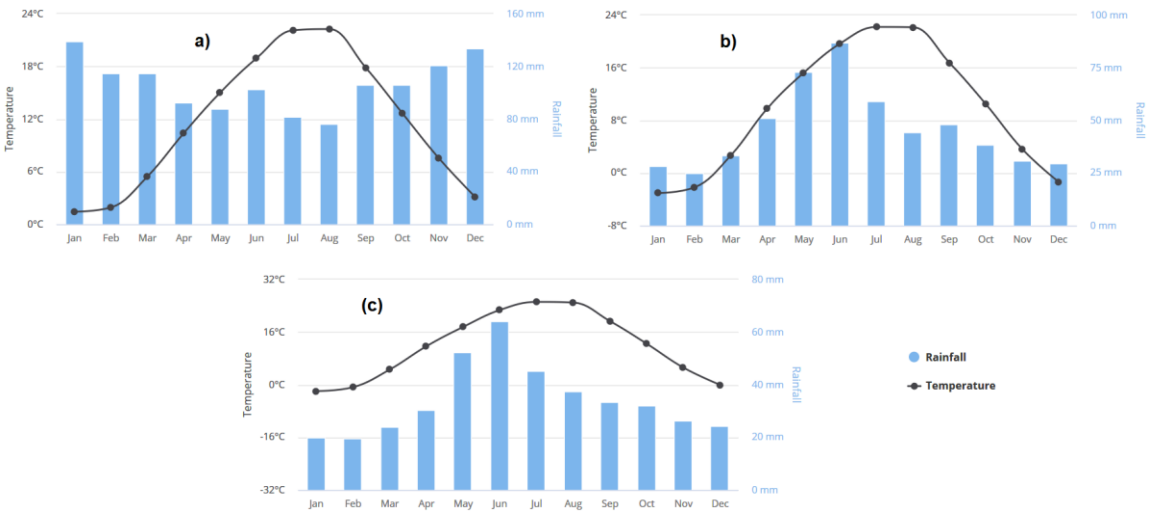

Figure 2. Averaged monthly temperature and rainfall for western **(a)**, central **(b)** and eastern parts **(c)** of investigated region in the period 1991–2016. Data source - World Bank, https://climateknowledgeportal.worldbank.org

3. Synoptic situation

The meteorological situation on 19 Aug 2015 over Northern Caucasus Districts of Russia was characterized by the influence of extensive surface ridge of high pressure stretched from the north, north-west and troughs at the south, accompanied with troughs at the north-east in the surface, middle and upper troposphere. A cyclonic depression was located along the Caucasian ridge and intensive west-east wind transport in a 200 km band between high pressure and trough (Figure 3).

The dominant circulation at 500 hPa was eastward with wind speed reaching 94 km/h at the 500 Mb level. Wind speed accrued with height and equaled 144 km/h at the level of 250 Mb (Figure 5). Such wind speeds in a cloud are confirmed by C- and S-band Doppler radar measurements (Figure 6g). The low- and middle levels winds transported warm and moist air masses from the Black Sea Coast towards the Northern Caucasus area as well as unstable atmospheric conditions (Figure 3 and 5).

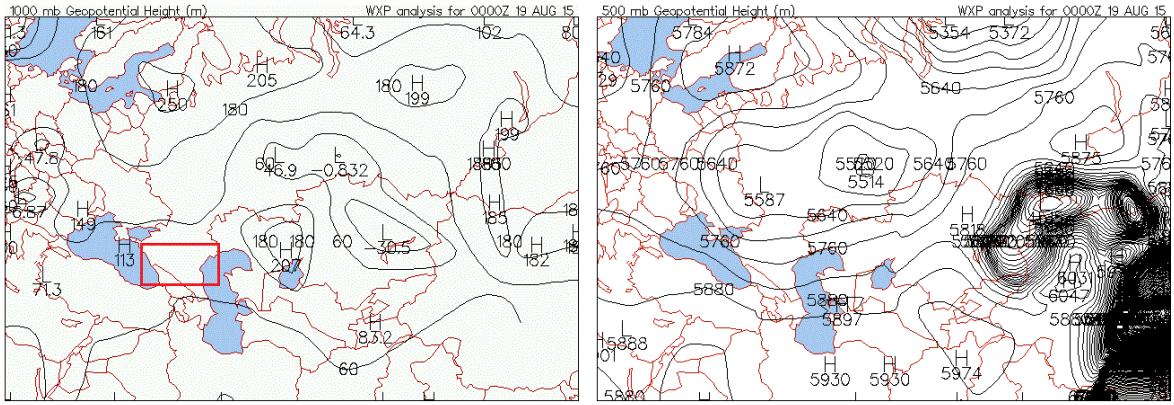

Figure 3. Upper air map of geopotential heights 1000 (left) and 500 (right) hPa at 0 UTC with analyzed area colored by red rectangle. Images are taken from the http://vortex.plymouth.edu/myo/upa/ctrmap-a.html.

Preprints (www.preprints.org) | NOT PEER-REVIEWED | Posted: 4 December 2019 doi:10.20944/preprints201912.0033.v1

4 .Upper Air Sounding

Upper air sounding data from the database of the University of Wyoming (http://weather.uwyo.edu/) is used in this study.

4.1 Area of analysis, bounded by a red rectangle, where development of investigated storms took place is represented in Figures 3 and 4. Three upper air sounding stations are located inside this area (Figure 4), they are: Tuapse (WMO Station Identifier 37011; 44.10ºN, 39.07ºE, and elevation 41.0m) which is on the west border, Divnoe (34858; 45.91ºN, 43.35ºE, 87.0m) - central north border and Mineralnye Vody (37055 URMM; 44.22ºN, 43.10ºE, 314.0 m) - central part. Skew-T datagrams, based on measurements which were carried out at mentioned stations are presented in Figure 5 for at 0 and 12 UTC (http://weather.uwyo.edu/upperair/sounding.html). Tables 1 and 2 contain derived indices of atmosphere instability and forecasts of storm probability and category. The dominating wind was from west to east.

Radiosondes at 0 UTC characterize atmospheric conditions prior to the formation of convective clouds. They first appeared at the western border of the studied area - the coast of Black Sea and sea area, while 12 UTC data corresponds to the supercell pass, after supercell and pass of second line of convective clouds (in dependence on time and location of sounding station).

Figure 4. Upper air sounding stations trapped into area of supercell analysis (red rectangle): 37011 – Tuapse, 34858 – Divnoe, 37055 URMM – Mineralnye Vody. Image taken from the http://weather.uwyo.edu/upperair/sounding.html

According to Tuapse station 1.5 km atmospheric boundary layer was particularly moist or nearly saturated with relative humidity 60-86% and absolute humidity qv=12.0-16.5 gkg^{-1}. Middle atmospheric level (up to 7.5 km) was also moist at 0 UTC (40-70%) and nearly saturated at 12 UTC (38-96%). Similar situation with relative humidity distribution was registered by two other stations, though mixing ratio was around 8.6-12.38 gkg^{-1} at Mineralnye Vody and 4.6-12.7 gkg^{-1} at Divnoe, it is significantly less than registered by Tuapse station. It can be explained by the fact that Tuapse is

Preprints (www.preprints.org) | NOT PEER-REVIEWED | Posted: 4 December 2019 doi:10.20944/preprints201912.0033.v1

located in the coastal strip while other stations are located in inland steppe (Divnoe) and foothill (Mineralnye Vody) areas.

Sounding conducted by Tuapse station at 0 UTC showed 4 inversion layers of different intensities from ground to the tropopause level. Boundary layer below 850 hPa, which is about 1.8km, was characterized by shallow inversion layer and nearly dry-adiabatic lapse rate in upper 1km layer. Convection inhibition slowly preventing formation of convective clouds at this time period was estimated as -30.3 J/kg. However measurements at 12 UTC showed that boundary inversion was broken making this layer unstable, while inversion near 4km level became stronger. Other 2 eastern stations showed strong inversion layers in the boundary layer and weak potential for cloud growth.

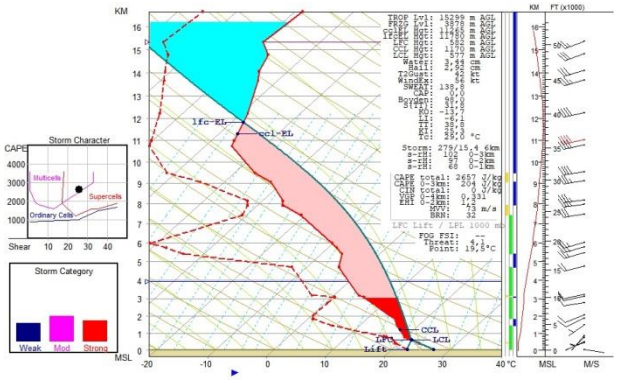

a) Tuapse (37011), 0UTC

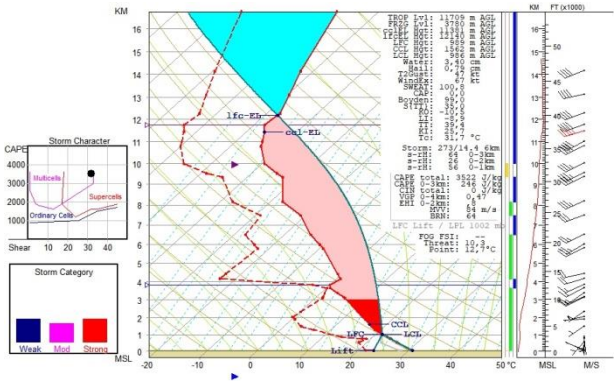

b) Tuapse (37011), 12UTC

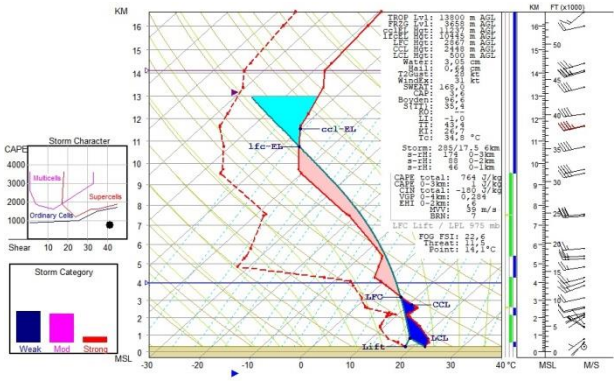

c) Mineralnye Vody (37055 URMM), 0UTC

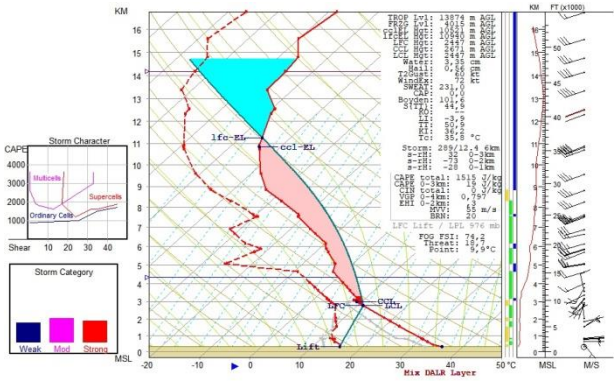

d) Mineralnye Vody (37055 URMM), 12UTC

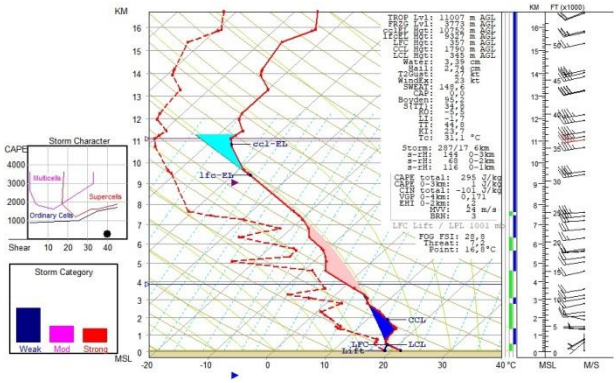

e) Divnoe (34858), 0UTC

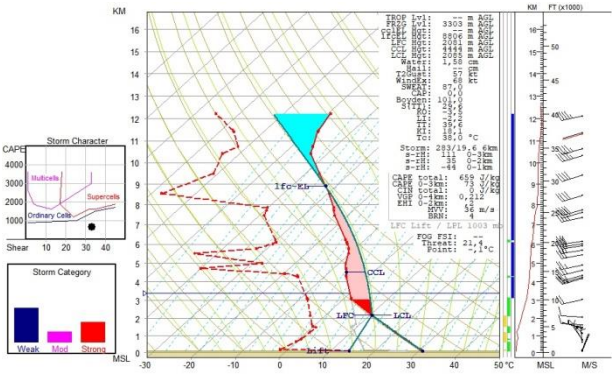

f) Divnoe (34858), 12UTC

Preprints (www.preprints.org) | NOT PEER-REVIEWED | Posted: 4 December 2019 doi:10.20944/preprints201912.0033.v1

Figure 5. SKEW-T diagrams for three stations: Tuapse (37011), Mineralnye Vody (37055 URMM) and Divnoe (34858), 19 Aug 2015, 0UTC (left side) and 12UTC (right side).

4.2 The analysis of atmospheric indexes derived from soundings for 0 and 12 UTC is presented below in Table 1. Calculated indexes for Tuapse station showed the highest probability of thunderstorm formation in comparison with the other two stations. Air temperature was very high with the daily maximum ranging between 30.0 and 33.0°C, this could potentially initiate the development of thunderstorm. Moreover, cumulus cloud development was favored due to very high humidity in atmospheric boundary layer; it that exceeds 80% at 0 UTC and 60% at 12 UTC, low deficit of dew point was registered.

Some of the atmospheric instability indexes were characterized by relatively high values, they did not reach the extreme values, but showed a potential for scattered severe storms development. Other indexes provided information about considerable levels of convective available potential energy (CAPE) and a high likelihood of extensive convective systems (K Index).

Analysis of radiosonde data of Tuapse station at 0 UTC showed (Tables 1 and 2) a development of single thunderstorms (KINX = 25.3), medium potential of convective instability (VTOT = 24.9). CAPE was equal to 2657 Jkg^{-1} at 0 UTC, it indicates the strong convective instability and probability of thunderstorm formation. 12 UTC sounding showed an increase in CAPE up to 3522 Jkg^{-1}, that indicates very high instability with probability of severe thunderstorms and tornadoes. Lifted index (Li = -8.9) denoted to high instability and probability of very strong thunderstorms. Lifting condensation level (1250m) is relatively low, indicates probability of convection development. Nevertheless, CTOT index was small (13.9) and do not predict thunderstorm, TTOT index (38.8) shows impossibility of thunderstorms, SWET index (140.56) also indicates absence of conditions for mature thunderstorms. There was considerable energy inhibiting convection, CIN amounts up to 58.63 Jkg^{-1}. The value of CIN would be higher, if the inversion layer occurred in the lower troposphere.

Table 1. Upper Air Sounding Indices and storm category forecast

Indices	Station name					
	Tuapse (37011)		Mineralnye Vody (37055 URMM)		Divnoe (34858)	
	0 UTC	12 UTC	0 UTC	12 UTC	0 UTC	12 UTC
KINX Instability Index	25.30	25.70	26.7	30.90	23.70	10.10
VTOT Vertical Totals	24.90	26.70	25.7	27.30	26.90	20.30
CTOT Cross Totals Index	13.90	12.70	17.7	18.30	17.90	11.30
TTOT Total Totals Index	38.80	39.40	43.4	45.60	44.80	31.60
SWET Severe Weather ThrEAT	140.56	101.08	168.22	181.25	147.65	83.53
Li Lifted index	-6.1	-8.9	-1.0	-3.3	1.37	14.89
CAPE Convective Available Potential Energy	2657	3522	764	1294	295	659
SHOW Showalter index	6.04	6.00	2.73	1.37	2.76	11.67
Convective Inhibition	-30.31	-58.63	-180	0	-339.16	0.00

Preprints (www.preprints.org) | NOT PEER-REVIEWED | Posted: 4 December 2019 doi:10.20944/preprints201912.0033.v1

Equilibrium Level	235.83	243.45	282.31	291.55	552.54	No value
Level of Free Convection	800.00	796.77	645.37	602.82	613.14	No value
Temp [K] of the Lifted Condensation Level	292.23	290.67	286.94	280.49	288.60	269.67
Pres [hPa] of the Lifted Condensation Level	923.38	885.90	870.55	726.25	943.03	756.50
Precipitable water [mm] for entire sounding	34.14	33.52	30.19	31.72	33.59	15.90
Storm Category Forecast	**Moderate**	**Strong, Supercells**	**Weak to Moderate**	**Moderate**	**Weak**	**Weak, Ordinary cells**

Table 2. Upper Air Sounding Indices for Station Tuapse, 12 UTC

	Station Tuapse (37011), 12 UTC	
Indices	Value	Forecast
KINX	25.70	Lightning storms with probability 70%
VTOT Vertical Totals	26.70	Moderate potential of convective instability and probability of lightning storms
CTOT Cross Totals Index	12.70	Troposphere has a low potential for convective instability, which is insufficient for thunderstorm activity.
TTOT Total Totals Index	39.40	Thunderstorm activity is not possible.
SWET Severe Weather ThrEAT	101.08	No conditions for the occurrence of severe thunderstorms
Li Lifted index	-8.9	High instability. Very strong thunderstorms
CAPE Convective Available Potential Energy	3522	Very strong instability (strong and very strong thunderstorms, tornadoes).
Showalter index	6.00	Weak general thunderstorm (instability) indicators
Convective Inhibition	-58.63	Weak to medium inhibition
Precipitable water [mm] for entire sounding	33.52	Heavy precipitation

4.3 According to the forecast, a development of convective clouds and single thunderstorm was expected. The development of a high depth hail thunderstorm was not expected due to small vertical temperature gradients and the absence of cold fronts.

5. Weather Radar Data

Several radars are installed in different parts of the investigated area. Some of the radars provided data each 10 minutes while others - each 3.5 minutes depending on the main purpose of their exploitation (storm warning, hydrology or hail suppression). These data provided possibility to track supercell storm from its origin at the coast of Black Sea to the coast of Caspian Sea, which Cb reached to the end of the day, though according to satellite data the supercell crossed the Caspian

Preprints (www.preprints.org) | NOT PEER-REVIEWED | Posted: 4 December 2019 doi:10.20944/preprints201912.0033.v1

Sea and invaded to neighboring country Kazakhstan. We acknowledge this limitation of the data from these storms.

Special software package suite ASU-MRL [4] was implemented for processing weather radars data, assimilation of satellite-lightning data and output of different radar products on the background of administrative map, as well as terrain map. Advanced tools and algorithms available within this system make possible to produce temporal courses of about 50 different characteristics of the clouds in forms of images and tables.

According to data of dual-wavelength (S/X band) radar MRL-5 and Dual-Polarization Doppler radars DMRL-C and DMRL-10 [5] of Krasnodar, Stavropol and North Caucasian Antihail Services of Russian Hydrometeorological Service (Roshydromet), from 1020 to 2000 UTC, a powerful supercell hailstorm with right-hand development [6] was observed and covered an ample territory of the North Caucasus. Two severe fast-moving (60-75km/h) supercells and several weaker hail clouds were tracked by radars (Figure 6a-b). However, here we focus on the first supercell which was the most developed one.

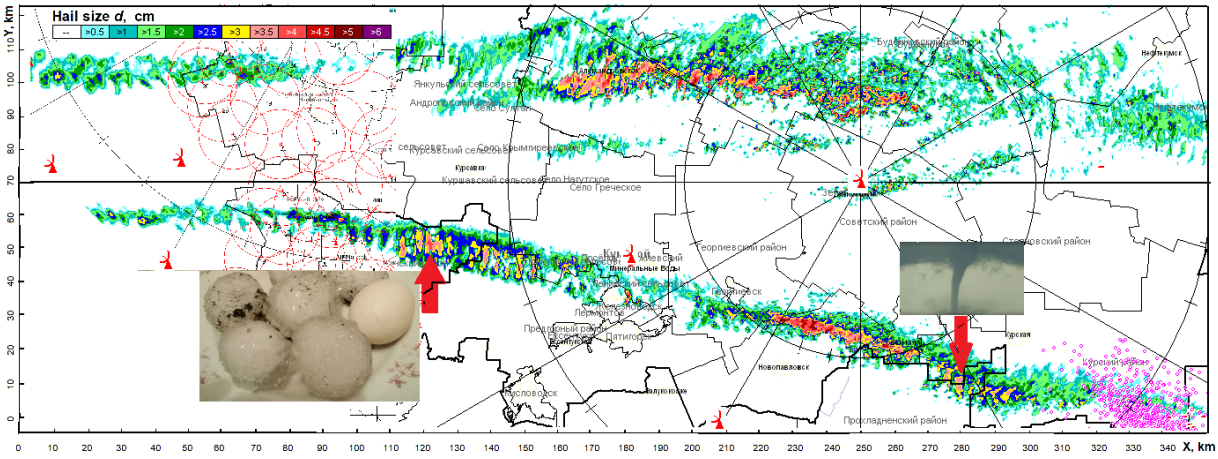

a)

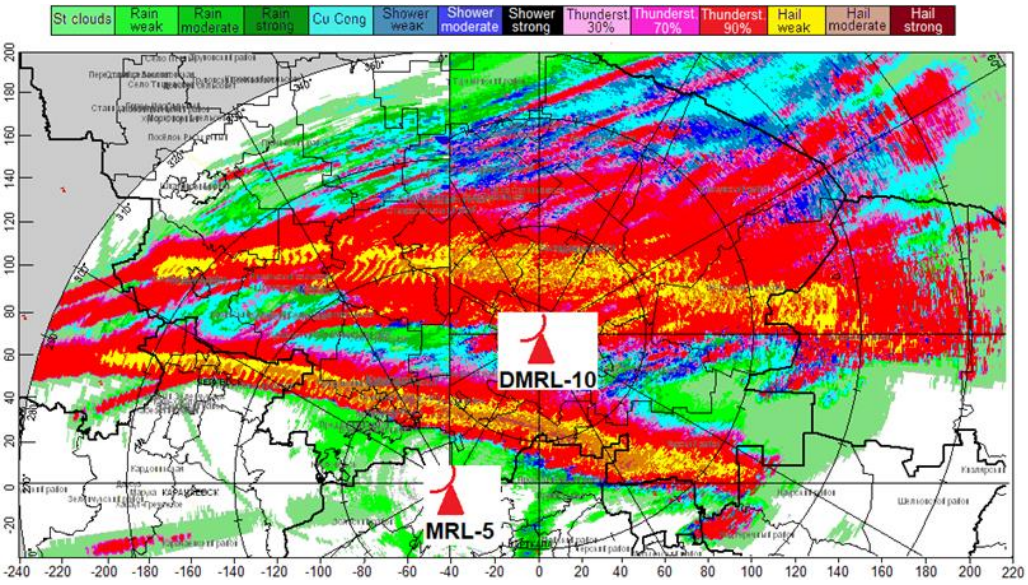

b)

Preprints (www.preprints.org) | NOT PEER-REVIEWED | Posted: 4 December 2019 doi:10.20944/preprints201912.0033.v1

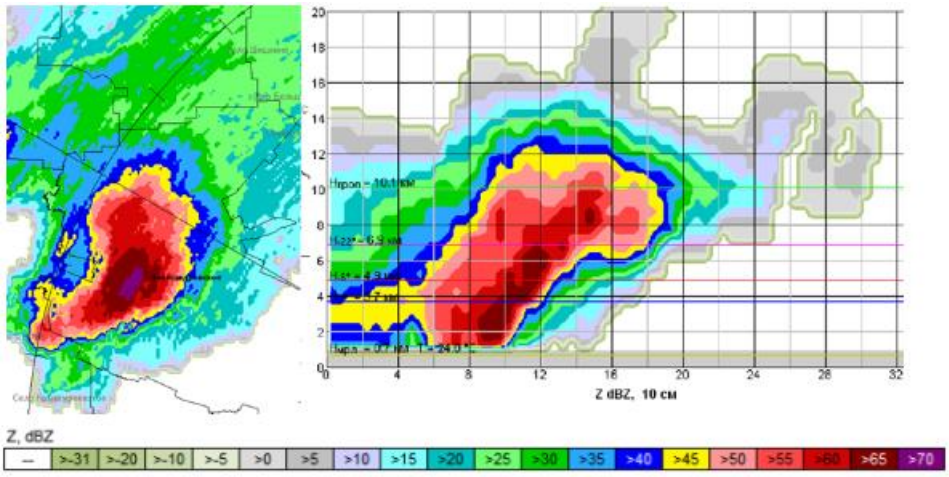

(c)

Figure 6. Characteristics of the supercell Cb cloud: **(a)** hail swaths and tornado; **(b)** accumulated meteorological phenomena; **(c)** pseudo-horizontal section on altitude 8 km (on the left) and vertical cross-section along the direction of radar echo overhang (on the right). Vertical and horizontal axes are distances in km.

The first supercell Cb formed on the territory of Adygea Republic, and with periodic strengthening and weakening, remaining in the quasi-stationary state of development, crossed the territory of several Districts and counties of the Northern Caucasus (Figure 1).

The map of meteorological phenomena integrated over time according to radar data is shown in Figure 6b. Radar echo structure at the peak of supercell development is presented in Figure 6c, which shows that the supercell had large overhang with radar reflectivity greater than 65 dBZ over area of weak radar echo. The bottom edge of overhang had altitude about 6 km. This indicates the presence of powerful updraft, which contributes to the formation of large hail with size in some places up to 6 - 7 cm.

From 1020 to 1852 UTC supercell Cb traveled about 635km almost straight east with a speed of movement 65-85km/h. Periodic amplification and weakening of the cloud was observed.

Analysis of the spatial structure and dynamics of the development of hail clouds have shown that they can be classified as supercells with right-hand development, moving to the right from the direction of the leading stream (40 - 50 degrees) with speed 50-90 m/sec in different periods (Figure 7g). Highly developed radar echo canopies were located on the right and windward flanks of the cloud system. The maximum values of radar characteristics were observed at 1258 UTC in the area of the village Sovetskaya of Krasnodar District, where radar reflectivity exceeded Z_{max} = 70 dBZ (Figure 7a), top of the clouds reached 15-16km (Figure 7b), and the upper boundary of the hail core - 11.2km. Cloud volume estimated by reflectivity greater than 15 dBZ at the peak of its development was nearly 10^5 km^3 (Figure 7c). Vertically integrated liquid reached extreme value 120 kg/m^2 (Figure 7d), while rain intensity (Figure 7e) was 500-600mm/h. The hail size on most of the hail path was about 2–3cm, and it reached 4–6 cm at times of maximum development (Figure 7f). The total duration of the supercell hailstorm was more than 10.5 hours (from 1020 to 2100 UTC, when it went out of the range of weather radars belonging to Roshydromet and invaded the territory of neighboring Kazakhstan.

Preprints (www.preprints.org) | NOT PEER-REVIEWED | Posted: 4 December 2019 doi:10.20944/preprints201912.0033.v1

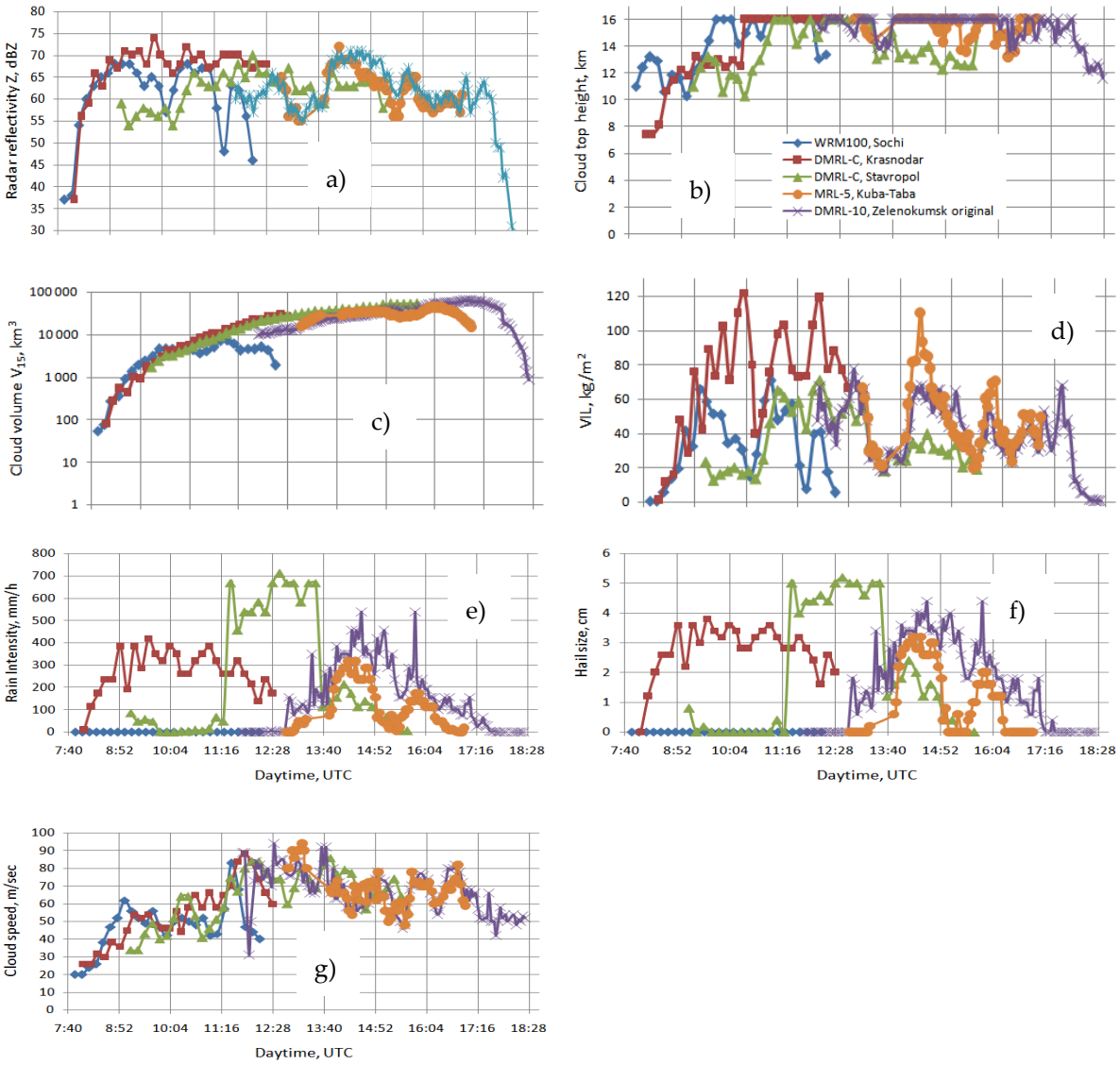

Figure 7. Radars derived characteristics of the supercell Cb cloud: **(a)** maximum radar reflectivity factor Z; **(b)** Cloud top height; **(c)** Cloud volume with reflectivity exceeding 15 dBZ; **(d)** VIL; **(e)** Rain intensity; **(f)** Hail size; **(g)** Cb propagation speed. Here WRM100 and DMRL-C - Dual-Pol C-band Doppler radars, DMRL-10 - S-band Doppler radar and MRL-5 - dual-wavelength S/X band radar.

6. Lightning Data

The simple conceptual model of the gross charge of thunderclouds, which has prevailed to the present, is based on dipole/tripole structure, as may be seen in comprehensive review of the charge distribution of storms by Williams [7]. In this context dipole/tripole refers to vertically separated, oppositely charged regions. However actual thunderstorms charge distribution usually is more complex than a simple dipole/tripole [8]. Some electric fields profiles measured by vertical soundings through storms have been so complex that it is doubtful that even gross structure of the charge distribution should be approximated as a dipole or tripole. In frames of this block we will be concentrated more on the frequency of positive and negative discharges produced by supercell and measured instrumentally rather than on considering the theory behind their formation.

Preprints (www.preprints.org) | NOT PEER-REVIEWED | Posted: 4 December 2019 doi:10.20944/preprints201912.0033.v1

The High Mountain Geophysical Institute (Nalchik, Russia) provided us with lightning detecting data to give geographic and temporal spread of lightning flashes for the area of the South of Russia. The lightning detection system installed in the North Caucasus [9] (Figure 8) consists of four LS8000 stations manufactured by Vaisala (Finland) and a central information receiving and processing center , which provides the acquisition, processing, and archiving of the lightning discharge data (coordinates, polarity, discharge type, currents, etc.). Each station has two sensors - low frequency (LF) and high frequency (VHF). The low-frequency LF sensor detects mainly lightning discharges of cloud-to-ground type. The high-frequency VHF sensor detects dominantly discharges of the cloud-to-cloud and intracloud type. Detection range for different types of lightning discharges is different. For the cloud-to-ground discharges, the maximum range is 625 km from the network center, and it is 325 km for the cloud-to-cloud discharges. The LS8000 system allows to determine the location of the lightning discharge with an accuracy ± 300 m; lightning discharge polarity with an accuracy 100%; lightning current values with an accuracy 10%; discharge time - 12%; the classification of discharges types (cloud-to-cloud, cloud-to-ground) with an accuracy close to 100%. However, joint analysis of the lightning and radar data [10, 11] has shown that flashes detection accuracy is estimated as 5 to 10 km, which is satisfactory for current analysis. In spite of this, the complex relief of the Caucasus seems to impair the quality and completeness of lightning data, but this fact has not been studied by us.

Figure 8. Scheme of lightning detection system, 4 red circles denote to positions of lightning sensors LS8000 and black isocontour bounds maximum area of signal detection.

Maximum frequency of cloud-to-ground (CG) discharges was fixed at 1420 UTC both for negative (Figure 9a) and positive (Figure 9b) flashes, reaching about 30-35min^{-1} and 60-70min^{-1} correspondingly. The frequency of discharges began gradually decline after that, and no discharges were measured after 17 UTC. However, this could be the result of both: weakening of the cloud and its departure from the zone of reliable detection by LS-8000. Here, it should be noted that the lightning data is related to the volume of the cloud detected by weather radars, i.e. those lightning flashes that are outside the radar echo are filtered. The frequency of cloud-to-cloud (CC) discharges is significantly higher (Figure 9c) reaching values 300-500min^{-1} at the peak of the supercell

Preprints (www.preprints.org) | NOT PEER-REVIEWED | Posted: 4 December 2019 doi:10.20944/preprints201912.0033.v1

development. An important fact is that the maximum frequency of discharges of different types (CG, CC) coincides in time, showing that the nature of all discharges is very similar. Total current of the CG discharges (Lf+) of positive and negative (LF-) polarities is almost identical in magnitude and differs by sign. It equals to 200-300 kA at the peak of development. Second-order polynomial trends obtained for the curves have a satisfactory correlation with data points, poorly describing the peak values of the characteristics at the time of their maximum, and correlate well with data points during development and dissipation stages. There is need to mention, that the beginning of the storm development was poorly measured due to the big distance from available sensors, much beyond area of reliable detection. We acknowledge this limitation of the data from this storm.

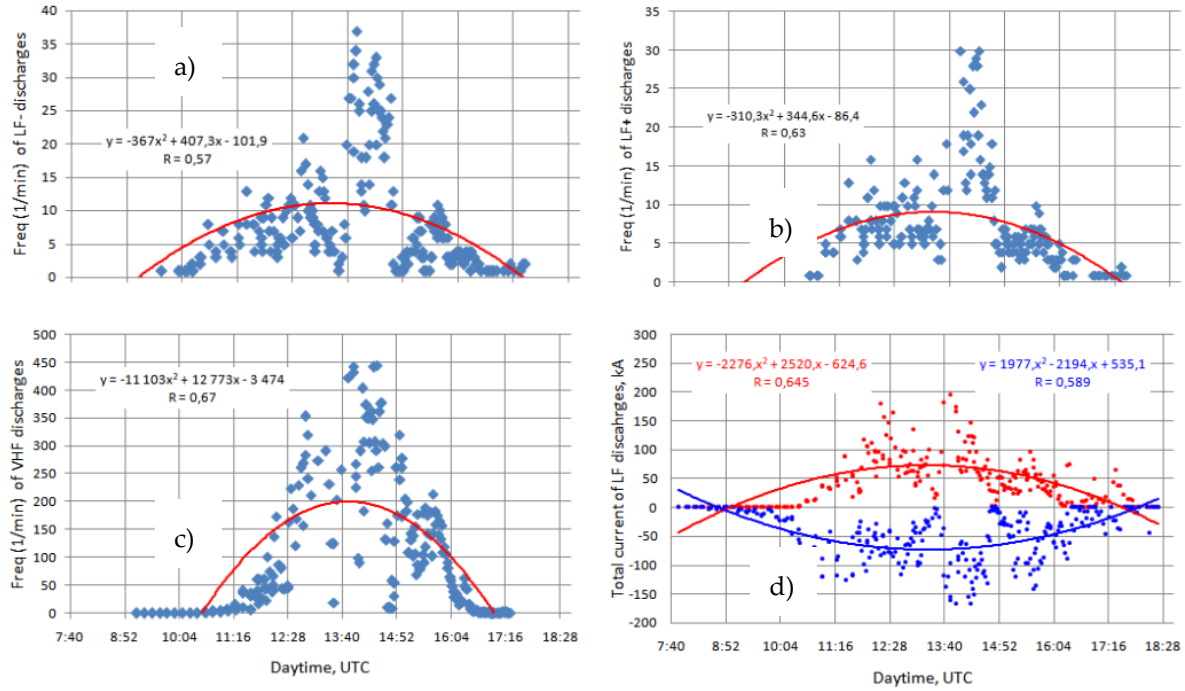

Figure 9. Lightning characteristics of supercell Cb with polynomial trends: **(a)** Frequency (min^{-1}) of negative LF-; **(b)** positive LF+; **(c)** VHF discharges (c); **(d)** Total current of cloud-to-ground discharges of positive LF+ (red) and negative LF- (blue) polarities. Here LF denotes to cloud-to-ground discharges and VHF to inter-cloud discharges.

7. Satellite Data

Satellite observations show that studied supercell Cb was formed at 0727 UTC in the coastline of Black Sea. Satellite imageries for different time periods are presented in Figure 10. They were derived from Meteosat-10 measurements at 10.8 μm channel.

Preprints (www.preprints.org) | NOT PEER-REVIEWED | Posted: 4 December 2019 doi:10.20944/preprints201912.0033.v1

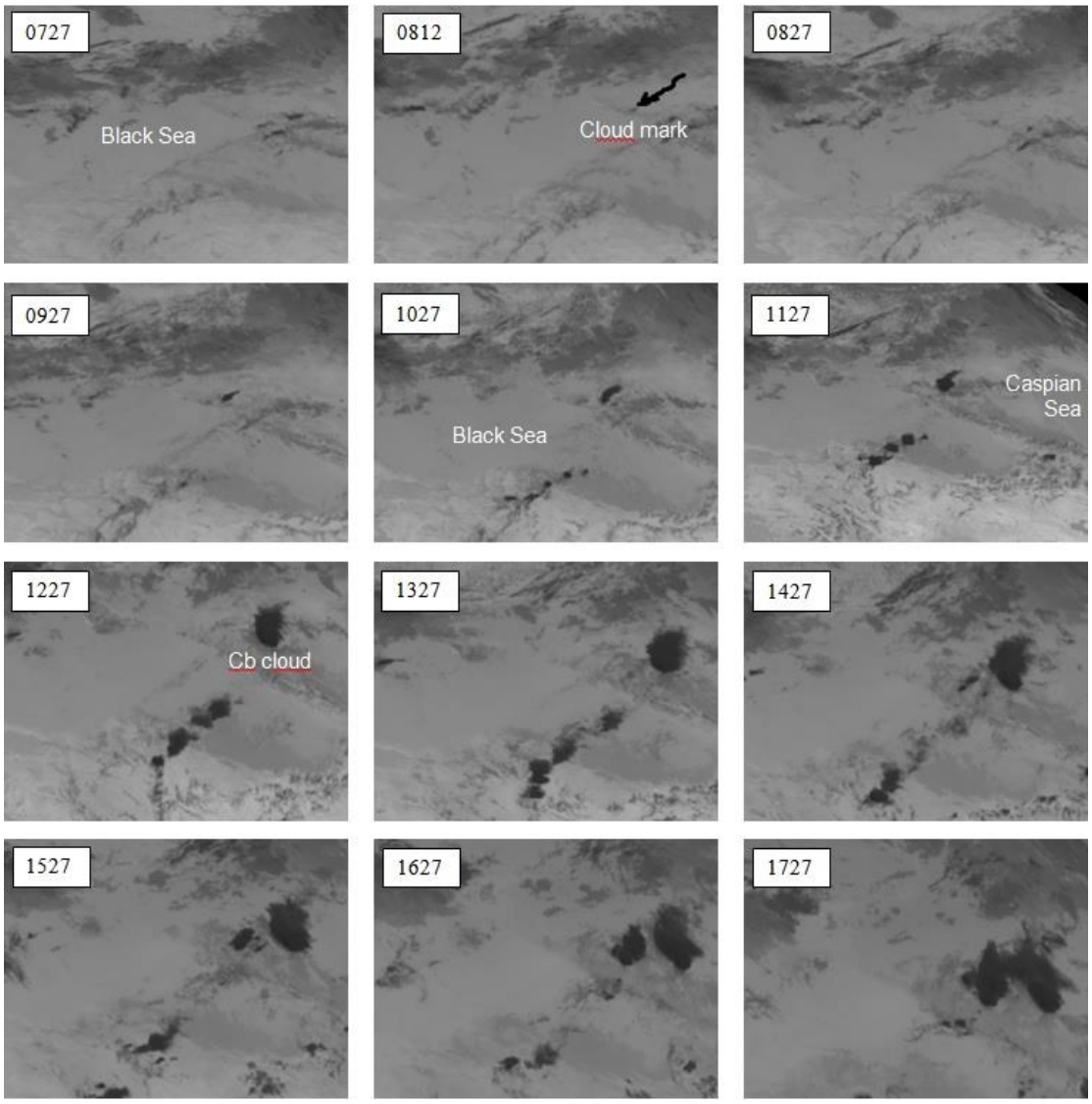

Figure 10. Tracking of supercell Cb cloud on Meteosat-10 (10.8μm channel) satellite imageries

Radiation temperature at 10.8 μm is presented in Figure 11a, which shows that minimum value on the top of the supercell cloud makes up about -60ºC at 12 UTC. Cb top height can be estimated using vertical temperature profile from radiosonde data at the nearest station Tuapse 37011 (Figure 5b). The maximum height of the cloud top is estimated as 17 km ASL, which is comparable to radar data (Figure 7b). It is seen that the minimum temperature decreased to 12 UTC, which indicates an increase in the height of the top.

The position of the cloud top is found using split technology (split-window technique). Difference between the radiation temperatures of the pixels corresponding to the clouds was determined in the radiometer channels 6.2 and 10.8 μm and then its maximum value was found as max(dif = $T_{6.2}$ - $T_{10.8}$); The position of the pixel with the maximum of this difference (Figure 11b) was taken as the position of the top of the cloud [12, 13].

Almost the same height of cloud top is obtained using 10.8 μm channel itself, where the pixel with minimum radiation temperature is assumed to be associated with cloud top. According to Figure 11f cloud top is increasing from 4 km at 0715 UTC to 17 km at 12 UTC.

Preprints (www.preprints.org) | NOT PEER-REVIEWED | Posted: 4 December 2019 doi:10.20944/preprints201912.0033.v1

Figure 11c shows number of pixels with ice (blue curve), liquid (red) and mixed (green) phases, from which we know that maximum glaciation of supercell top occurred approximately at 1500 UTC.

Data from multispectral measurements using a SEVERI radiometer, installed on a satellite, was used to assess precipitation intensity IMVtop. The minimum radiation temperature T_{min} at the top, measured in the atmospheric 10.8 μm window, was used to calculate precipitation intensity. It was determined by the regression ratio between precipitation intensity and temperature at the cloud top [12]. It is based on the relationship between the height of the top and the intensity of precipitation, which increases with increasing cloud thickness by formula:

$$IMV_{top} = 3.524*10^{13}*Exp(-0.133* T_{min}), \quad (1)$$

The intensity of precipitation was in the range 20-150 mm/hour(Figure 11d). The maximum intensity was recorded at 1536UTC.

Figure 11e shows precipitation flux. Most intensive flux (22000 m^3/sec) was observed at 15UTC. Assessments of rain intensity based on radar measurements show that it amounts up to 550 mm/h (Figure 7e) of the mixed phase precipitation. Hail size was 4.5cm at this moment (Figure 7f).

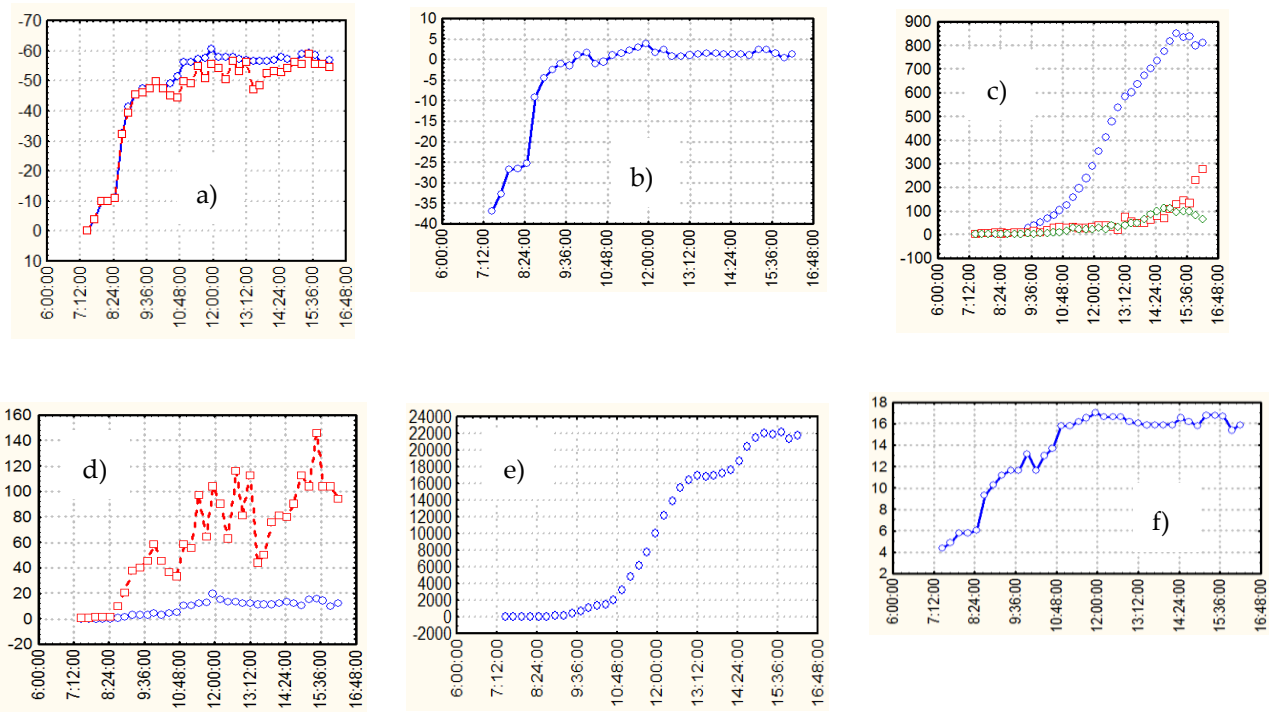

Figure 11. Satellite derived characteristics of the supercell Cb cloud: **(a)** Radiation temperature - absolute minimum (blue) and cloud top (red); **(b)** Max temperature difference in channels 6.2 and 10.8 μm; **(c)** Number of pixels with ice (blue), water (red) and mixed phase (green); **(d)** Precipitation intensity, mm/h - maximum (red line) and average (blue) in the pixel corresponding to cloud top; **(e)** Total cloud precipitation flux, m^3/sec; **(f)** Cloud top height estimated by satellite 10.8 m infrared channel and upper-air sounding (Tuapse station); horizontal axis denotes to UTC time.

8 Combined data analysis

Radar-satellite-lightning data was synchronized temporally and spatially and then inserted into one map or chart. For radar-lightning analysis all lightning flashes that occurred between two

Preprints (www.preprints.org) | NOT PEER-REVIEWED | Posted: 4 December 2019 doi:10.20944/preprints201912.0033.v1

consequent radar scans were retrieved, then the frequency of lightning was calculated by dividing their number on time in minutes between radar scans. This usually implies that a lightning discharge has occurred within a radius of several kilometers from the boundary of cloud. For the sake of consistency, we have chosen only those discharges which coexisted geographically with radar reflectivity of the investigated cloud greater than 5 dBZ, while others flashes were excluded from analysis.

8.1 Interlinks between radar and lightning characteristics

In this section, we analyzed correlation relationships between various radar derived characteristics and the intensity of lightning discharges of the supercell cloud. The better correlation (R=0.7) was found for pair V_{45} (km^3) and intensity of LF discharges (Figure 11c). A slightly weaker correlation (0.63) was obtained for intensity of VHF discharges (Figure 11d). Nearly the same correlation was found for pair Z_{max} and intensity of VHF discharges (0.66) (Figure 11b), and (0.5) for LHF discharges (Figure 11a). Weaker correlation was found between cloud volume having radar reflectivity exceeding 35 dBZ and intensity of LF (0.436) (Figure 11e) and VHF (0.44) (Figure 11f) discharges. Correlations between precipitation intensity and intensity of LF and VHF discharges had coefficients 0.45 and 0.57 respectively (Figure 11g-h).

Such relatively weak to moderate correlations may indicate the fact that the 5 radars, which data was utilized in this analysis, have different measurement errors associated with the influence of complex terrain, different wavelengths and antenna beamwidth, calibrations, etc. The main error in measuring lightning characteristics in this case is the large distance of the supercell from the registration stations (see Figure 8), especially during its development stage near the Black Sea. In the absence of the indicated errors, our opinion is that the correlations should be higher.

Preprints (www.preprints.org) | NOT PEER-REVIEWED | Posted: 4 December 2019 doi:10.20944/preprints201912.0033.v1

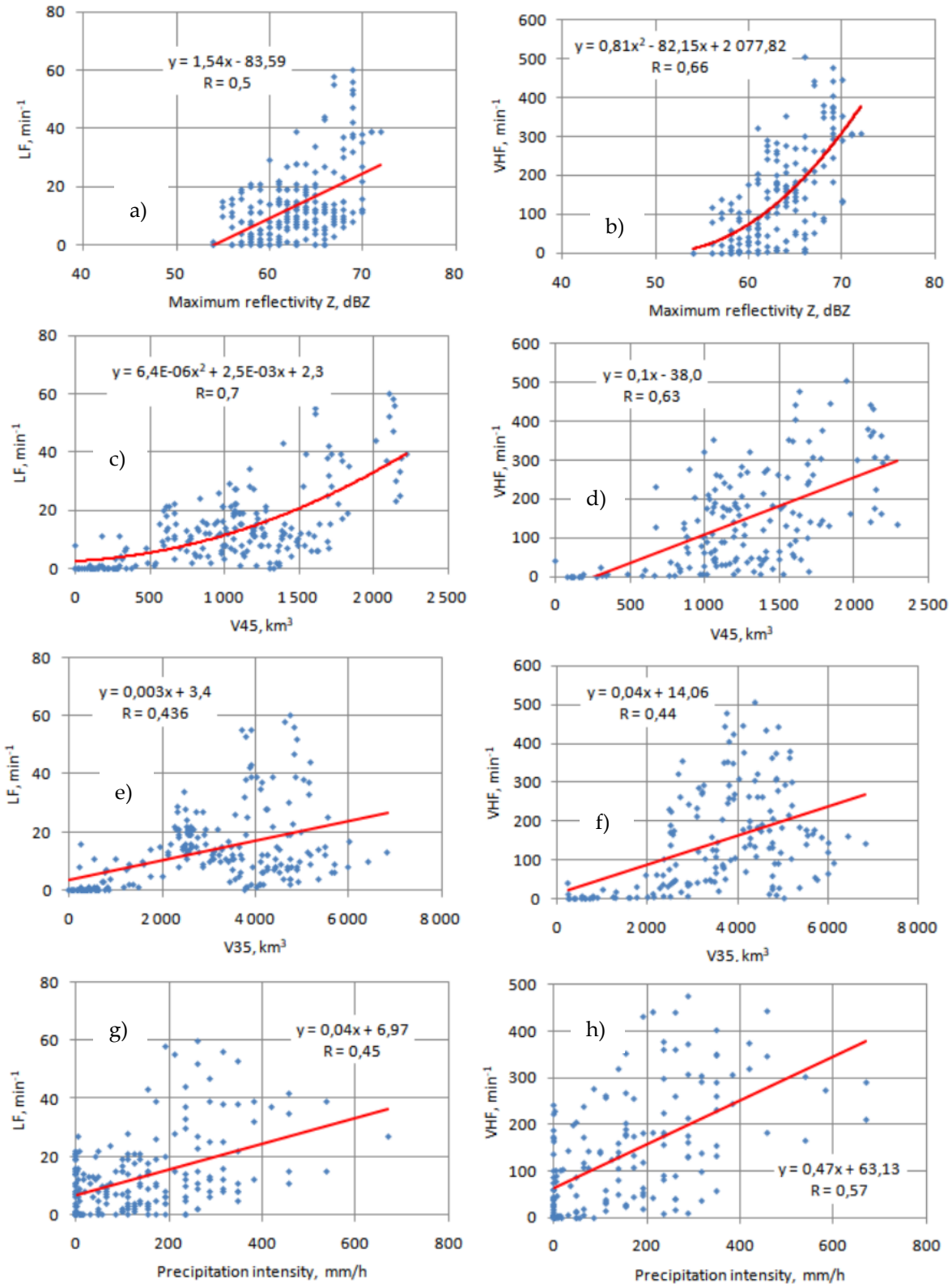

Figure 12. Correlations between radar and lightning characteristics of the supercell Cb cloud - Dependence of LF (left column) and VHF (right column) discharges frequency from: **(a-b)** maximum radar reflectivity Z; **(c-d)** cloud volume with radar reflectivity exceeding 45 dBZ; **(e-f)** cloud volume with radar reflectivity exceeding 45 dBZ; **(g-h)** precipitation intensity.

Preprints (www.preprints.org) | NOT PEER-REVIEWED | Posted: 4 December 2019 doi:10.20944/preprints201912.0033.v1

8.2 Interlinks between satellite, radar and lightning characteristics

In this block, to assess the trends of all types of data and their consistency, we tried to combine the following parameters together on the same time chart - lightning frequency for cloud-to-cloud and cloud-to-ground flashes, satellite derived cloud top temperature and precipitation intensity, radar derived vertically integrated liquid and cloud volume with reflectivity exceeding 45 dBZ (Figure 12).

It can be seen from the graph that all these parameters grow, stagnate and decrease in unison, especially radar and satellite characteristics. Radar derived characteristics reached their maximums earlier than maximum of lightning activity. Lightning characteristics have some delay in their increase at the stage of cloud growth and more quickly fall out in the stage of dissipation, though it may be a result of the bigger distance between the cloud and zone of reliable signal reception for this period.

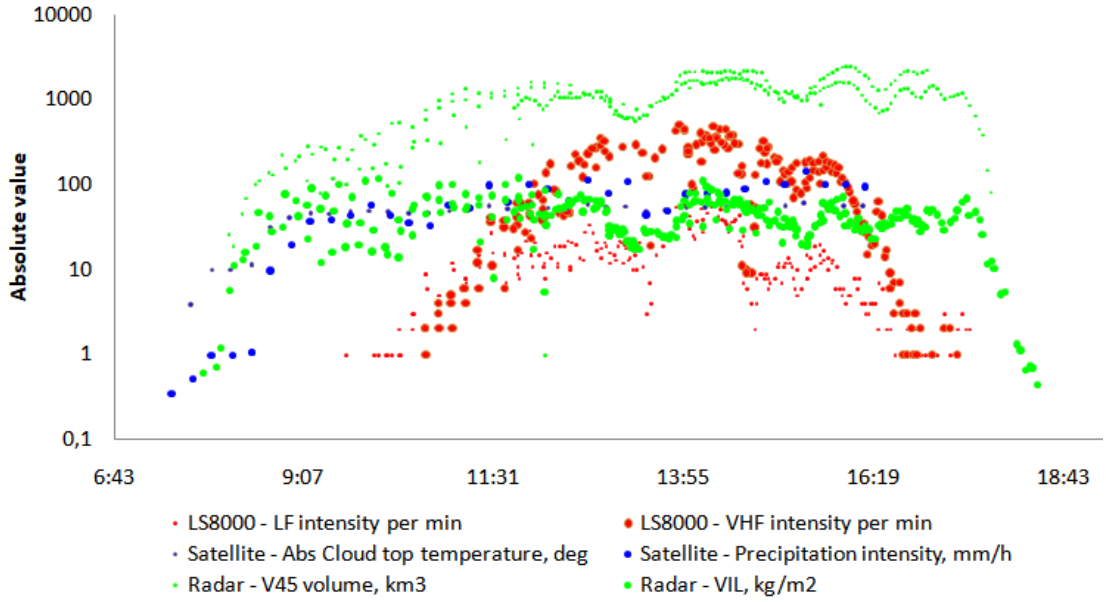

Figure 13. Combined temporal characteristics of lightning, satellite and radar-derived parameters: red dots and circles denote to minute intensity of lightning discharges of LF and VHF types by LS8000 system; blue - absolute cloud top temperature in degrees Celsius and precipitation intensity by Meteosat-10 data; green - cloud volume with radar reflectivity exceeding 45 dBZ and VIL.

9 Hail

According to radar data, hail existed almost continuously throughout the period of Cb existence, except 20-30 min after its appearance (Figure 7f). It can be noted that in 1 hour after the cloud was formed, the hail size was already 4-5 cm. Further, the hail size oscillated within the mentioned limits for 7.5 hours and only then began to decrease. Such a long hail existence makes it possible to obtain some estimates of the relationship between hail size and lightning activity of the cloud (Figure 14). These estimates show that thunderstorm activity increases generally for both cloud-to-ground (Figure 14a) and intracloud (Figure 14b) discharges with increasing hail size, the dependencies are moderate (R = 0.46 - 0,59). A weaker dependence (0.39) is obtained for the pair hail size - total current of LF discharges (Figure 14c).

Preprints (www.preprints.org) | NOT PEER-REVIEWED | Posted: 4 December 2019 doi:10.20944/preprints201912.0033.v1

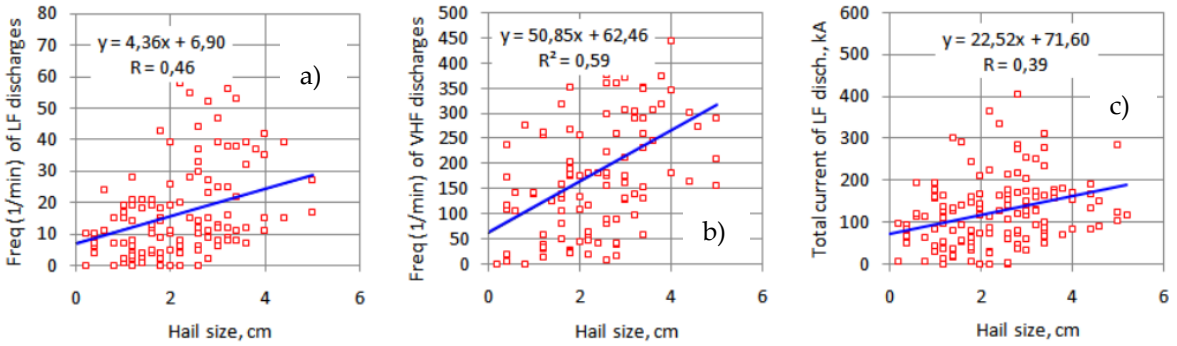

Figure 14. Relationship between maximum hail size and frequency of LF **(a)** and VHF **(b)** discharges, total current of LF discharges in kA **(c)**. Blue lines and y(x) formulas represent trends, while R2 - accuracy of approximation.

10 Tornado

According to media sources and eyewitness observations it is known that the cloud at certain periods had a narrow funnel-shaped upward flow, similar to a tornado shape. However, no well-documented ground data on tornado existence was found, and further conclusions of this block are based on Doppler-polarimetric radar analysis, which usually offer remarkable insight into the dynamics and microphysics of convective storms.

The dual-polarization variables that were utilized are radar reflectivity factor at horizontal polarization (Z_{HH}), differential reflectivity (Z_{DR}), the magnitude of the copolar cross-correlation coefficient [$|\varrho_{HV}(0)|$; herein ϱ_{HV}], Doppler velocity (v_r), and specific differential phase (K_{DP}). For a review of the polarimetric variables and the utility of polarimetric radar data in meteorological applications, see, for example [14-15].

Tornadic debris signature (TDS) is mainly governed by debris loft having randomly orientated particles. Irregular shape, large size and high dielectric constant of debris results in high Z_H, low Z_{DR}, and anomalously low ϱ_{HV} [16]. In our case Z_H exceeded 60 dBZ (Figure 15-16a), $Z_{DR} > -1$ dB (Figure 15-16b), $\varrho_{HV} < 0.6$ (Figure 15 - 16d) in the investigated case. TDS is usually collocated with the tornado vortex signature (TVS) [14, 17]. TVS is marked on figure 17. It is located in the same place as TDS. Extreme Doppler velocity reached values -43 and +63 m/s. In addition prominent radar echo hook [18] was easily identified in 1 km layer above the ground (Figure 15a).

Intense local convergence zone in the near-surface layer produces strong updraft which then sucks insects and/or other light debris, including grass, leaves, or dust. This debris is characterized by irregular shapes and random orientation, which contribute to the drop in ϱ_{HV} [16]. Inflow signature is marked on figure 15c.

Z_{DR} columns in supercells are relatively narrow (4–8 km wide) (Figure 15b) and typically extend several kilometers above the environmental freezing level and are indicative of a positive temperature perturbation associated with the updraft. The high values of Z_{DR} (>3 dB) indicate the presence of large, oblate hydrometeors, presumably either large raindrops or water-coated hailstones [16]. In this case Z_{DR} column is not very deep, with top located on 4.5 km (Figure 16b).

The Z_{DR} arc is observed as a low-level (<2 km above ground level), arc-shaped region of high Z_{DR} (>3 dB) located along the gradient of Z_H on the inflow side of the forward flank of supercell

Preprints (www.preprints.org) | NOT PEER-REVIEWED | Posted: 4 December 2019 doi:10.20944/preprints201912.0033.v1

(Figure 15). It is hypothesized to appear as a result of strong size sorting in the presence of strong veering wind shear in supercell environments [15].

At low levels, an area of enhanced K_{DP} (Figure 15-16d) is often observed within the heavy precipitation core of supercells, called the "K_{DP} foot" [19]. Though it largely overlaps the Z_H core, K_{DP} is less sensitive to large hail and thus is a better indicator of heavy rain and small melting hail. Thus, the K_{DP} foot may be a better indicator of the downdraft regions, at least those driven by rain evaporation and hail melting.

TDS, TVS, Z_{DR} column, Z_{DR} arc, and K_{DP} foot were observed during the entire period (1130 – 1433 UTC) when the supercell was in the near zone of the radar (< 120 km). Inflow was observed from 1333 to 1433 UTC.

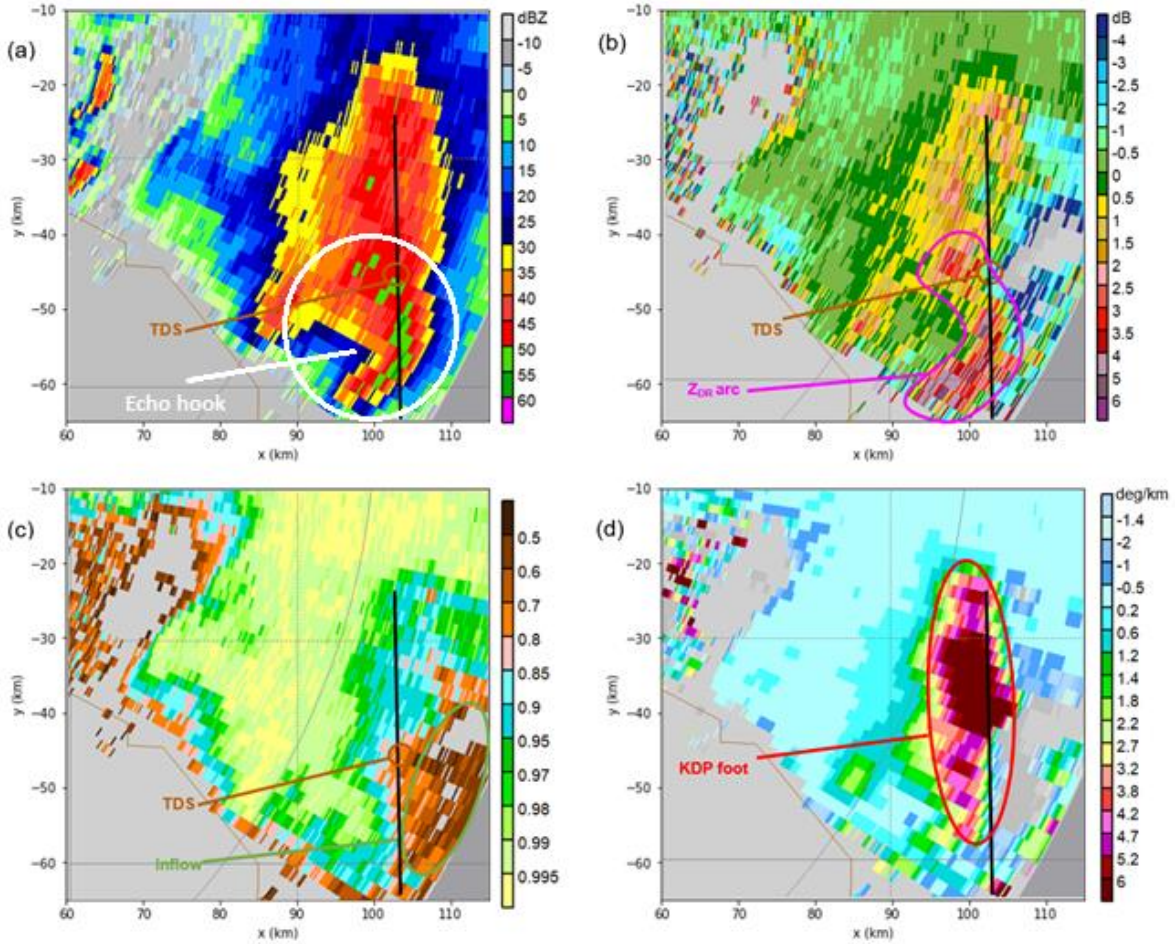

Figure 15. Four-panel display of the 1 km level at 1433 UTC by DMRL-C radar near Stavropol: **(a)** Z_H, **(b)** Z_{DR}, **(c)** ρ_{HV}, and **(d)** K_{DP}.

Preprints (www.preprints.org) | NOT PEER-REVIEWED | Posted: 4 December 2019 doi:10.20944/preprints201912.0033.v1

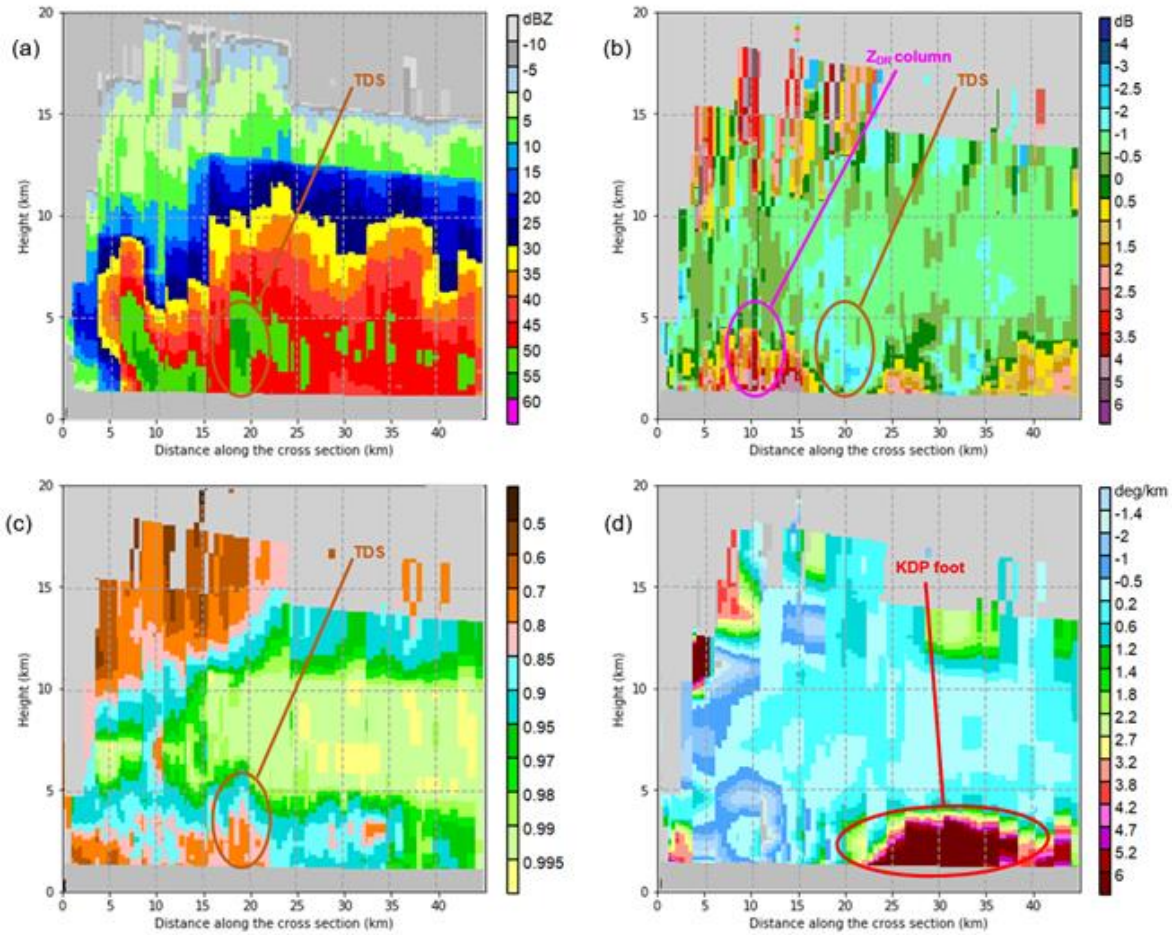

Figure 16. Vertical cross section of **(a)** Z_H, **(b)** Z_{DR}, **(c)** ρ_{HV}, and **(d)** K_{DP} corresponding to black line (shown in Figure 15).

Preprints (www.preprints.org) | NOT PEER-REVIEWED | Posted: 4 December 2019 doi:10.20944/preprints201912.0033.v1

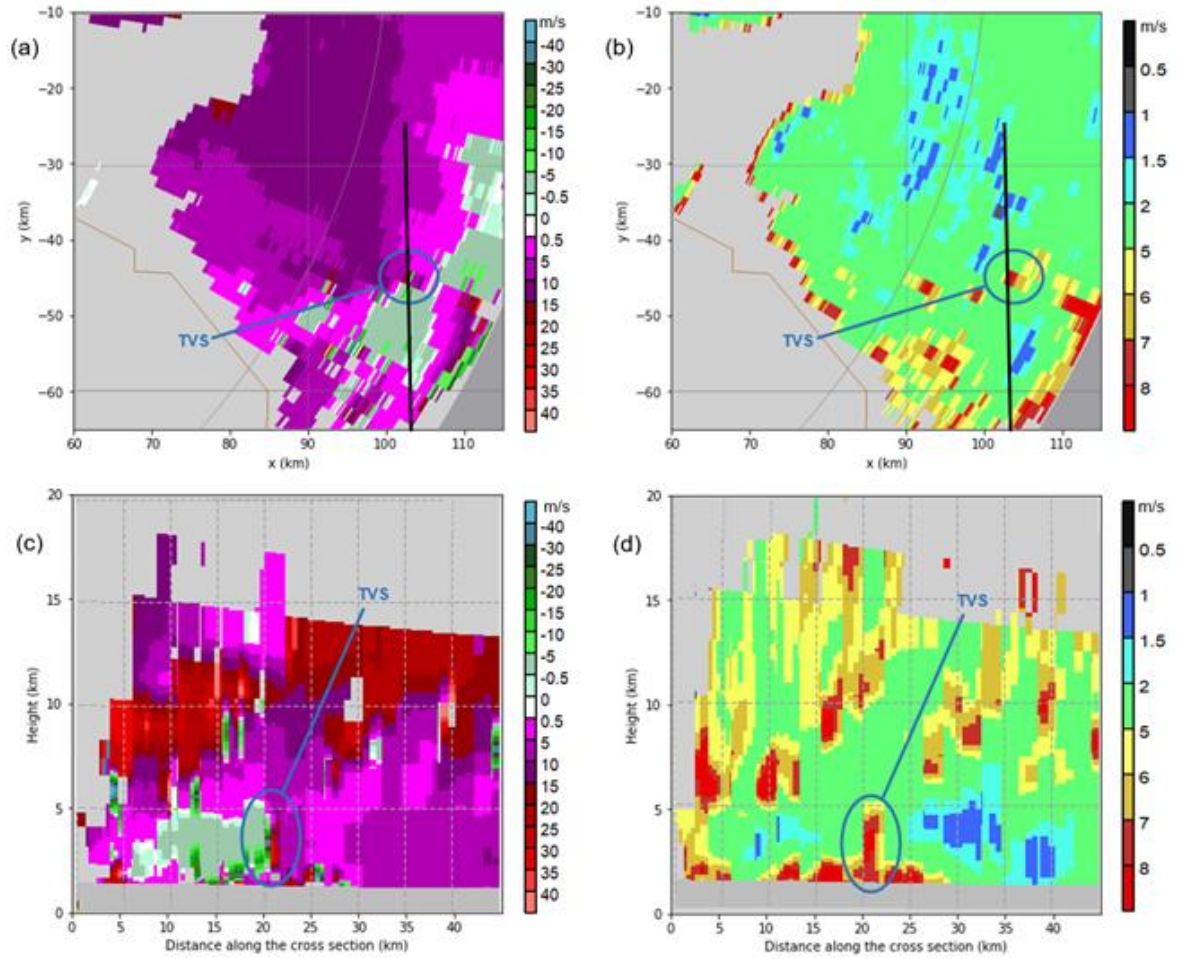

Figure 17. Fields of **(a)** Doppler velocity V, and **(b)** spectrum W at altitude 1 km above ground at 1433 UTC, and **(c)** vertical cross section of V, and **(d)** W, corresponding to the black line (shown in Figure 15).

11 Conclusions

A combinatorial analysis of the case study of supercell thunderstorm developed on 19 Aug 2015 in the Northern Caucasus was carried out. Radiosonde, satellite, radar and lightning data were utilized for this analysis. The main aim of this study was to identify common patterns in the lightning regime and its interrelations with other cloud characteristics. Main results of this study are formulated below:

1. The supercell was right-hand development, moving to the right from the direction of the leading stream (40 - 50 degrees) with speed 50-90 m/sec in different periods. The maximum value of radar reflectivity was about 75 dBZ, cloud top - 15-16km, and the upper boundary of the hail core - 11.2km. Cloud volume estimated by reflectivity greater than 15 dBZ at the peak of its development was nearly 10^5 km^3. VIL reached extreme value 120 kg/m^2, while rain intensity - 500-600mm/h. The hail size on most of the hail path was about 2–3cm and 4–5cm at times of maximum development. The total duration of the supercell hailstorm was more than 10.5 hours (from 1020 to 2100 UTC, when it went out of the range of weather radars belonging to Roshydromet and invaded the territory of neighboring Kazakhstan.

 doi:10.20944/preprints201912.0033.v1

2. Tuapse (37011) radiosonde station, located on the Black Sea coast, showed the highest probability of thunderstorm formation in comparison with other stations. Air temperature was high with the daily maximum 30-33°C, cloud development was favored due to very high humidity (80% at 0 UTC) in boundary layer. Some of the atmospheric instability indexes were characterized by relatively high values and did not reach extreme values, but showed potential for single storms development (KINX = 25.3) and medium potential of convective instability (VTOT = 24.9). CAPE was equal to 2657 Jkg^{-1} at 0 UTC and 3522 Jkg^{-1} at 12UTC, that indicates very high instability with probability of severe thunderstorms and tornadoes. Lifted index (Li = -8.9) denoted to high instability and probability of very strong thunderstorms. Nevertheless, CTOT index was small (13.9) and failed to predict thunderstorm, TTOT index (38.8) showed impossibility of thunderstorms, SWET index (140.56) also indicated absence of conditions for mature thunderstorms. There was considerable energy inhibiting convection (CIN = 58.63 Jkg^{-1}).

3. The quadratic approximations of time dependence of frequency of lightning flashes are determined for the whole lifetime of the supercell. The best fit is found for the cloud-to-cloud flashes (R = 0.67), while the lowest for cloud-to-ground flashes of negative polarity (R = 0.57). Accumulated current of cloud-to-ground flashes of both polarities has correlationcoefficient 0.59 - 0.65;

4. Lightning data can be used for approximate computing of thunderstorm track providing estimates of speed, direction and distance travelled, quick-and-dirty prediction of cloud development and dissipation;

5. Analysis of relationships between radar-derived characteristics and lightning frequency revealed moderate approximation with cloud volume V_{45} (R = 0.7 for LF and 0.63 for VHF discharges), which suggests that lightning activity can be well predicted by this parameter;

6. Correlations between lightning frequency and precipitation intensity (I, mm/h) are moderate to weak (0.45 for LF and 0.57 for VHF discharges). That may reflect the fact that 5 radars utilized in this analysis have different measurement errors associated with the influence of complex terrain, different wavelengths and antenna beamwidth, calibrations, etc. The main error in measuring lightning characteristics in this case is the large distance of the supercell from the registration stations, especially during its development stage near the Black Sea Coast. In the absence of the indicated errors, our opinion is that the correlations should be higher;

7. Long period of hail existence have made it possible to estimate relationship between hail size and lightning activity. It was found that an increase in lightning activity for flashes of all types is directly proportional to the increase in hail size, though the coefficient of correlation is moderate to weak (0.46 - 0.59). Very similar dependencies were found for vertically integrated liquid, precipitation intensity and cloud volumes bounded by radar reflectivity's 35 and 45 dBZ;

8. Characteristics obtained with the help of radars and satellite reached their maximums earlier than maximum in lightning activity. This fact support an idea that electrical processes are secondary and appear as a result of complex chain of cloud microphysical and dynamical processes;

9. In the absence of radar and lightning measurements, satellite data can be applied to roughly estimate the cloud top height, maximum precipitation flux and predict frequency of lightning flashes;

10. Doppler-polarimetric radar data revealed strong inflow zone from 1333 to 1433 UTC and confirmed tornado observations by eyewitnesses. At this tornadic debris signature collocated in space with tornado vortex signature was manifested by radar reflectivity factor Z_H> 60 dBZ,

differential reflectivity Z_{DR} > -1 dB, copolar cross-correlation coefficientρ_{HV} < 0.6m. Doppler velocity in mesocyclone zone varied from -43 to +63 m/s. Prominent radar echo hook was clearly identified in 1.5 km layer above the ground. Z_{DR} columns were relatively narrow (4–8 km wide) and not very deep (4.5 km).

Although the results are encouraging, there are wide areas for further improvements and explorations. To better utilize retrieved characteristics of various data types (such as satellite, radar, lightning), accurate data selection, bad data filtering and errors measurement techniques are needed for better fitting the observations with all sets of control variables.

Author Contributions: conceptualization and writing—review and editing, M.T.A.; writing—original draft preparation, methodology, A.M.A; formal analysis, supervision, Y.P.M.; funding acquisition, writing—review and editing, A.A.S.; investigation – tornado analysis, V.B.P.; lightning data curation, A.K.A.

Funding: This research was funded by Russian Foundation for Basic Research (RFBR), grant number 18-55-80020 and 17-05-00965

Conflicts of Interest: Authors have no competing interests to declare. Any opinions, findings and conclusions or recommendations expressed in this material are those of the author(s) and do not necessarily reflect the views of the Russian Foundation for Basic Research, funder of the research.

Acknowledgments: The radiosonde and satellite data used in this manuscript is publicly available at the online Data Pools of the University of Wyoming and EUMETSAT. Radar and lightning data were courteously provided by Central Aerological Observatory (Moscow) and High Mountain Geophysical Institute of the Russian Hydrometeorological Service. The authors thankfully acknowledge all technicians, engineers, and meteorologists who were responsible for collecting the primary data, for maintaining and calibrating the instruments and the technical systems that served as the data sources in this analysis.

References

1. Beck, H.E., Zimmermann, N.E., McVicar, T.R., Vergopolan, N., Berg, A., Wood, E.F., 2018: Present and future 374 Köppen-Geiger climate classification maps at 1-km resolution. Sci. Data, 5, 180214.
2. Peel, M.C., Finlayson, B.L., McMahon,T.A., 2007: Updated world map of the Köppen-Geiger climate 376 classification. Hydrol. Earth Syst. Sci., 11:1633-1644.
3. The World Bank Climate Change Knowledge Portal 2.0 Available online: 378 http://sdwebx.worldbank.org/climateportal/ (accessed on Jan 27, 2019).
4. Abshaev, M.T., Abshaev, A.M., Malkarova, A.M., Zharashuev, M.V., 2010: Automated radar identification, measurement of parameters, and classification of convective cells for hail protection and storm warning. Russian Journal Meteorology and Hydrology, 2010, No 35: p. 182. https://doi.org/10.3103/S1068373910030040.
5. Abshaev, M.T., Abshaev, A.M., Efremov, V.S., Vilegjanin, I.S., 2015: New radars for research and seeding of clouds.Proc. of the 2 Int.Sci.Conf., Stavropol, 2015. Pp. 265-270.
6. Abshaev, A.M., Abshaev, M.T., Malkarova, A.M., Barekova, M.V., 2014: Guidelines for the organization and conduct of antihail works, Nalchik, Printing house.508 p.
7. Williams, E.R., 1989: The tripole structure of thunderstorms. J. Geophys. Res., 94, 13,151-13,167.
8. Macgorman, Donald & Rust, W. & Williams, Earle. (1999). The Electrical Nature of Storms. Physics Today - PHYS TODAY.52. 10.1063/1.882670.
9. Adzhiev, A.H., Stasenko, V.N., Tapaskhanov,V.O., 2013: Lightning detection system in the North Caucasus. Russian Journal Meteorology and Hydrology, No 38. https://doi.org/10.3103/S1068373913010019.

10. Mikhailovskii, Y.P., Sin'kevich A.A., Pawar S.D. et al., 2017: Investigations of the development of thunderstorm with hail. Part 2.Analysis of methods for the forecast and diagnosis of the electrical properties of clouds.Russian Journal Meteorology and Hydrology. No 42.377. https://doi.org/10.3103/S1068373917060036.
11. Adzhiev, A.H., Kuliev, D.D., 2018: Characteristics of Storm Activity and Parameters of Lightning Discharges in the South of the European Part of Russia, Izv. Atmos. Ocean. Phys. No 54: 372. https://doi.org/10.1134/S0001433818040187.
12. Kraus, V.V., Sinkevich, A.A., Ghulam, A.S., 2012: Measurement of high intensity precipitation using remote sensing methods. Russian Journal Meteorology and Hydrology, 2012, No 7.Pp. 15-27.
13. Kurino, T., 1997: A satellite infrared technique for estimating deep/shallow precipitation. Advances in Space Research, vol.19 (3).Pp.511–514.
14. Ryzhkov A.V., Zrnic D. S. Radar Polarimetry for Weather Observations. Switzerland: Springer, 2019.486 p.
15. Kumjian, M. R. 2013: Principles and applications of dual-polarization weather radar. PartII: Warm-and cold-season applications. J. Operational Meteor., 1 (20), 243-264.
16. Kumjian, M. R. and A. V. Ryzhkov, 2008: Polarimetric signatures in supercell thunderstorms. J. Appl. Meteor. Climatol., 47, 1940–1961.
17. Brown, R. A., Lemon, L. R., & Burgess, D. W. (1978). Tornado detection by pulsed Doppler radar. Monthly Weather Review, 106,29–38.
18. Markowski, P.M., 2002: Hook echoes and rear-flank downdrafts: A review. Mon. Wea. Rev., 130, 852–876.
19. Romine, G.S., D.W. Burgess, and R.B. Wilhelmson, 2008: A dual-polarization-radar-based assessment of the 8 May 2003 Oklahoma City are a tornadic supercell. Mon. Wea. Rev., 136, 2849–2870